THE JOURNAL OF BIOLOGICAL CHEMISTRY VOL. 290, NO. 51, pp. 30406–30416, December 18, 2015

Carboxyl-terminal Truncations of ClC-Kb Abolish Channel Activation by Barttin Via Modified Common Gating and Trafficking*

Received for publication, June 30, 2015, and in revised form, October 5, 2015 Published, JBC Papers in Press, October 9, 2015, DOI 10.1074/jbc.M115.675827

Gabriel Stölting[1], **Stefanie Bungert-Plümke, Arne Franzen, and Christoph Fahlke**[2]

From the Institute of Complex Systems 4 (ICS-4), Zelluläre Biophysik, Forschungszentrum Jülich, 52425 Jülich

Background: Carboxyl-terminal truncations of hClC-Kb cause Bartter syndrome.
Results: hClC-Kb channels lacking the carboxyl terminus still associate with barttin, but are neither stabilized in the membrane nor activated.
Conclusion: Truncated hClC-Kb channels are not regulated by barttin.
Significance: Elucidating the role of the carboxyl terminus of hClC-Kb significantly improves our understanding of CLC-K regulation by barttin.

ClC-K chloride channels are crucial for auditory transduction and urine concentration. Mutations in *CLCNKB*, the gene encoding the renal chloride channel hClC-Kb, cause Bartter syndrome type III, a human genetic condition characterized by polyuria, hypokalemia, and alkalosis. In recent years, several Bartter syndrome-associated mutations have been described that result in truncations of the intracellular carboxyl terminus of hClC-Kb. We here used a combination of whole-cell patch clamp, confocal imaging, co-immunoprecipitation, and surface biotinylation to study the functional consequences of a frequent *CLCNKB* mutation that creates a premature stop codon at Trp-610. We found that W610X leaves the association of hClC-Kb and the accessory subunit barttin unaffected, but impairs its regulation by barttin. W610X attenuates hClC-Kb surface membrane insertion. Moreover, W610X results in hClC-Kb channel opening in the absence of barttin and prevents further barttin-mediated activation. To describe how the carboxyl terminus modifies the regulation by barttin we used V166E rClC-K1. V166E rClC-K1 is active without barttin and exhibits prominent, barttin-regulated voltage-dependent gating. Electrophysiological characterization of truncated V166E rClC-K1 demonstrated that the distal carboxyl terminus is necessary for slow cooperative gating. Since barttin modifies this particular gating process, channels lacking the distal carboxyl-terminal domain are no longer regulated by the accessory subunit. Our results demonstrate that the carboxyl terminus of hClC-Kb is not part of the binding site for barttin, but functionally modifies the interplay with barttin. The loss-of-activation of truncated hClC-Kb channels in heterologous expression systems fully explains the reduced basolateral chloride conductance in affected kidneys and the clinical symptoms of Bartter syndrome patients.

The chloride channel (CLC)[3] family is a large gene family encoding anion transport proteins in virtually every living cell. There are nine human members: hClC-1, hClC-2, hClC-Ka, and hClC-Kb are anion channels, whereas hClC-3 through hClC-7 function as anion/proton antiporters (1). CLC channels and transporters exhibit a dimeric structure with two separate conduction pathways (protopores) (2) or active centers (3), respectively. In CLC channels, this architecture results in the occurrence of two structurally distinct gating processes: fast protopore gating that opens and closes individual protopores independently of the adjacent subunit and common gating that acts jointly on both subunits.

hClC-Ka and hClC-Kb share a sequence homology of ~91% and are both predominantly expressed in renal and inner ear epithelial cells (1, 4, 5). An accessory subunit, barttin, is necessary for proper trafficking, protein stability and activation of both human CLC-K channels (6). Although hClC-Ka and hClC-Kb expression shows significant overlap, it is assumed that these two chloride channels exert distinct cellular functions. hClC-Ka participates in the transepithelial sodium chloride reuptake along the thin ascending limb of Henle facilitating water reabsorption in the adjacent thin descending limb of Henle whereas hClC-Kb predominantly mediates the basolateral chloride efflux necessary for salt absorption in the thick ascending limb of Henle (7–9).

The differences in localization and physiological function of the two human renal chloride channels are reflected in separate symptoms of human diseases that are caused by naturally occurring mutations in *CLCNKA* (encoding ClC-Ka) or *CLCNKB* (encoding ClC-Kb). *CLCNKA* mutations were associated with high blood pressure (10) or heart failure (11). In contrast, loss-of-function of hClC-Kb results in Bartter syn-

* This work was supported by the Deutsche Forschungsgemeinschaft (FA301/10-1, to Ch. F.). The authors declare that they have no conflicts of interest with the contents of this article.
[1] To whom correspondence may be addressed: Institute of Complex Systems 4 (ICS-4) – Zelluläre Biophysik, Forschungszentrum Jülich, 52425 Jülich, Germany. Tel.: +49-2461-61-4041; Fax: +49-2461-61-4216; E-mail: g.stoelting@fz-juelich.de.
[2] To whom correspondence may be addressed: Institute of Complex Systems 4 (ICS-4) – Zelluläre Biophysik, Forschungszentrum Jülich, 52425 Jülich, Germany. Tel.: +49-2461-61-4041; Fax: +49-2461-61-4216; E-mail: c.fahlke@fz-juelich.de.

[3] The abbreviations used are: CLC, chloride channel; hClC-Kb, human ClC-Kb channel; rClC-K1, rat ClC-K1 channel; CBS, cystathionine-β-synthase domain; GFP, green fluorescent protein.

drome type III, a genetic human disease condition characterized by hypokalemia, metabolic alkalosis, polyuria, polydipsia, and low blood pressure at increased levels of renin and aldosterone (9, 12, 13). There are several distinct forms of Bartter syndrome that are all due to loss-of-function mutations in proteins involved in salt resorption by the thick ascending loop of Henle (9, 14), *i.e.* in the apical Na^+-K^+-$2Cl^-$ symporter type 2 (NKCC2) (Bartter syndrome type I) (15), the apical potassium channel ROMK (type II) (16), the accessory subunit barttin (type IV) (17) as well as the calcium-sensing receptor (CaSR) (type V) (18, 19). When compared with these types of Bartter syndrome, patients with *CLCNKB* mutations often experience a less pronounced disease phenotype. Symptoms are usually detected at later ages and are often manageable with supportive treatment (20). The less severe phenotype of Bartter syndrome type III might be the result of the existence of an additional basolateral chloride efflux pathway, the potassium-chloride cotransporter KCC4, in the thick ascending limb of Henle (21), which might partly compensate loss of function of hClC-Kb channels.

So far, around 50 naturally occurring *CLCNKB* mutations have been identified in genetic screenings of patients with Bartter syndrome (22). Many of those result in truncations of the cytosolic carboxyl terminus within or nearby the two conserved cystathionine-β-synthase domains (CBS1 and CBS2) (20, 23–25). One of these truncation mutations, W610X hClC-Kb, is among the most prevalent *CLCNKB* mutations in asian populations (23–25). We here perform a detailed study of the functional consequences of this mutation on hClC-Kb and hClC-Kb/barttin function as well as the mechanism by which the ClC-K carboxyl terminus modifies ClC-K function and its regulation by barttin.

Experimental Procedures

Construction of Expression Plasmids, Mutagenesis, and Heterologous Expression—Coding regions of barttin, hClC-Kb, or V166E rClC-K1 were cloned into pcDNA3.1 or pRc/CMV vectors (Life Technologies GmbH, Darmstadt, Germany), with eGFP or mCherry linked to the amino terminus of the channels and mCherry or mYFP attached to the carboxyl terminus of barttin (6). Previous experiments demonstrated that constructs with and without attached fluorescent proteins behave similarly (6, 26–29). We therefore treated fusion proteins of full-length hClC-Kb with eGFP or mCherry as wild type (WT) channels, and simplified V166E eGFP-rClC-K1 to V166E rClC-K1 Truncation mutations were generated by inserting stop codons at the respective location using the QuikChange system (Agilent Technologies, Waldbronn, Germany) or overlapping extension PCR (30).

To study the effects of CLC-K truncations on channel expression, intracellular trafficking or function we used heterologous expression in two different cell lines, MDCKII and HEK293T cells (6, 26, 31). CLC-K/barttin function and subcellular distribution are comparable in both systems (6, 31). Robust expression and negligible background currents make HEK293T perfectly suited for functional characterization of WT and mutant CLC-K/barttin channels. For studies of channel localization and trafficking we used confluent MDCK II cells that are known to show epithelial properties such as cell polarization and proper sorting and trafficking (26, 32) while retaining the electrophysiological signature of ClC-K/barttin in HEK293T cells (31).

For biochemical experiments with hClC-Kb, HEK293T cells were co-transfected with 1 μg of pcDNA3.1 eGFP- or mCherry-hClC-Kb and 4 μg of pcDNA3.1 barttin-mCherry or -mYFP using the calcium phosphate technique (33). For all other experiments on hClC-Kb a combination of 1 μg of pcDNA3.1 eGFP-hClC-Kb and 2 μg pcDNA3.1 barttin-mCherry was used. Cells were split 24 h after transfection and used for experiments the following day. For the electrophysiological characterization of truncated or non-truncated V166E rClC-K1, 2 μg of pRc-CMV eGFP-V166E rClC-K1 was co-transfected together with 3 μg pcDNA3.1 barttin-mCherry. Cells were split 8 h after transfection and used for experiments the following day. For surface biotinylation experiments MDCK II cells were transfected using Lipofectamine2000 (Life Technologies) according to the manufacturer's protocol.

Whole-cell Patch Clamp and Data Analysis—Whole-cell patch clamp recordings were performed using an EPC10 amplifier controlled by the PatchMaster software (HEKA Elektronik, Lambrecht/Pfalz, Germany) as described (34). The external solution contained (in mM): 140 NaCl, 4 KCl, 2 $CaCl_2$, 1 $MgCl_2$, and 10 HEPES while the internal solution contained 115 NaCl, 2 $MgCl_2$, 5 EGTA, and 5 HEPES. Both solutions were adjusted to pH 7.4. Data were analyzed using FitMaster (HEKA Elektronik), Excel and Python 2.7. To obtain the voltage dependence of the relative open probability of full-length or truncated V166E rClC-K1 channels (Fig. 5), instantaneous current amplitudes were determined after a voltage step to +105 mV following prepulses to various voltages and plotted against the preceding potential. For WT and P683X/V166E rClC-K1/barttin current amplitudes were normalized to maximum values. For W534X and W610X rClC-K1/barttin amplitudes were scaled to match the lowest value of the full-length rClC-K1 V166E in the absence of barttin.

Unless noted otherwise, Student's *t* test was used for statistical comparison with * denoting $p < 0.05$ and **, $p < 0.01$. p values larger than 0.05 were considered non-significant and labeled "n.s."

Confocal Imaging—Cells were grown in ibidi μ-dishes and fixed prior to imaging with 2.5% para-formaldehyde dissolved in PBS. Imaging was performed on an inverted confocal laser scanning microscope (Leica TCS SP5, Leica Microsystems, Heidelberg, Germany) using a 63×/1.4 oil immersion objective. GFP was excited using a 488-nm laser and emission light was collected between 490 and 580 nm. mCherry was excited using a 594-nm laser, and the emission recorded between 596 and 680 nm.

Quantification of Protein Expression Levels—Membrane proteins were solubilized from 80% confluent Petri dishes of transfected HEK293T cells using ComplexioLyte 47a (Logopharm GmbH, March, Germany). The lysate was cleared by centrifugation at 13,000 × *g* at 4 °C. For quantification of expression levels, 40 μl of lysate was loaded on a 10% SDS gel.

Immunoprecipitation Experiments—400 μl of cleared lysates from transfected HEK293T cells were incubated with 1 μg of

monoclonal anti-GFP antibody for 1h (Life Technologies). The same amount of the cleared lysate was used as a control for unspecific binding and processed further without antibody. Antibody-bound proteins were purified on protein G-Sepharose beads by incubation for 2 h (Thermo Fisher Scientific, Braunschweig, Germany) and eluted using 50 μl of 2× SDS loading buffer. Samples were run on a 10%SDS gel and analyzed after fluorescence scanning. The signal from the lane without antibody incubation was considered as background and subtracted from the signal of the anti-GFP treated lane. Testing the specificity of the antibody with lysates from cells expressing mCherry-ClC-Kb or W610X mCherry-ClC-Kb alone did not give any signal in the antibody treated sample.

Surface Protein Biotinylation—Cell surface expression of hClC-Kb channels was investigated using a modification of cell surface biotinylation methods described previously (26, 35). MDCK II cells (10-cm dishes) were grown to confluency after transfection, washed with PBS, and incubated with 1 mg of EZ linked NHS-Sulfo-SS-biotin (Thermo Scentific) in PBS for 30 min. After quenching of free biotin with 10 mM glycine in PBS, cells were lysed using RIPA buffer, harvested, centrifuged at 16,100 × *g* for 15 min and then incubated with 150 μl pre-equilibrated NeutrAvidin beads (Thermo Scientific) for 1 h. Biotinylated proteins were eluted off the column with 2× SDS sample buffer. All steps were carried out at 4 °C. 30 μg of cell lysate and 50 μl of biotinylated proteins were run on a 10% SDS gel. Cells transfected with cytosolic mVenus were used as control to test the specificity of this biotinylation protocol to label surface membrane proteins.

Visualization and Quantification of SDS-PAGE Gels—Gels were scanned on a fluorescence gel scanner (Typhoon FLA 9500, GE Healthcare, Freiburg, Germany) at 100 μm resolution. GFP was excited at 473 nm, and the emission recorded using a 530/20 bandpass filter. The signal of mCherry was recorded using a 532 nm laser and a longpass 575-nm filter. Gel images were quantified using the Fiji software. Gels were rotated up to 3° using bilinear interpolation and subsequently quantified using the built-in tools for gel analysis.

Results

Deletion of CBS2 Results in Barttin-independent, Constitutively Active hClC-Kb Channels—Eukaryotic CLC proteins exhibit 18 transmembrane α-helices followed by a cytosolic carboxyl terminus, which contains two cystathionine-β-synthase domains (1, 36). A naturally occurring mutation that predicts truncation of hClC-Kb after the first CBS domain (W610X hClC-Kb) was found in patients with Bartter syndrome (Fig. 1*A*, *left*) (23, 25). To study the functional consequences of this mutation we expressed W610X hClC-Kb, either alone or together with the accessory subunit barttin (Fig. 1*A*, *right*), in mammalian cells and recorded currents through whole-cell patch clamping.

Fig. 1*B* depicts representative current responses to voltage steps from −145 to +135 mV from cells expressing WT or hClC-Kb W610X either without (left panel) or with barttin (*right panel*). In the absence of barttin, hClC-Kb did not show any activity (mean current at −105 mV: −0.09 ± 0.02 nA, n = 10 *versus* −0.09 ± 0.03 nA, n = 5 for untransfected HEK293T cells; p = 0.994). Co-expression with its accessory subunit barttin resulted in robust bi-directionally rectifying currents (at −105 mV: −1.22 ± 0.19 nA, n = 8; $p < 0.001$ *versus* hClC-Kb alone) (Fig. 1, *B* and *C*). Expression of W610X hClC-Kb resulted in visibly bi-directionally rectifying currents even in the absence of barttin (at −105 mV: −0.32 ± 0.06 nA, n = 11; $p < 0.001$ *versus* hClC-Kb alone) (Fig. 1, *B* and *C*). Cells co-expressing W610X hClC-Kb with barttin exhibited slightly larger mean current amplitudes than cells expressing the channel alone (at −105 mV: −0.71 ± 0.10 nA, n = 8; p = 0.02 *versus* hClC-Kb W610X alone). Previous biochemical and microscopic data have demonstrated that hClC-Kb inserts into the plasma membrane even in the absence of barttin (6, 26, 28). The absence of measurable currents from cells expressing WT hClC-Kb alone indicates that hClC-Kb remains inactive without barttin (6). In contrast, W610X hClC-Kb does not only reach the plasma membrane, but is active also in the absence of barttin. This

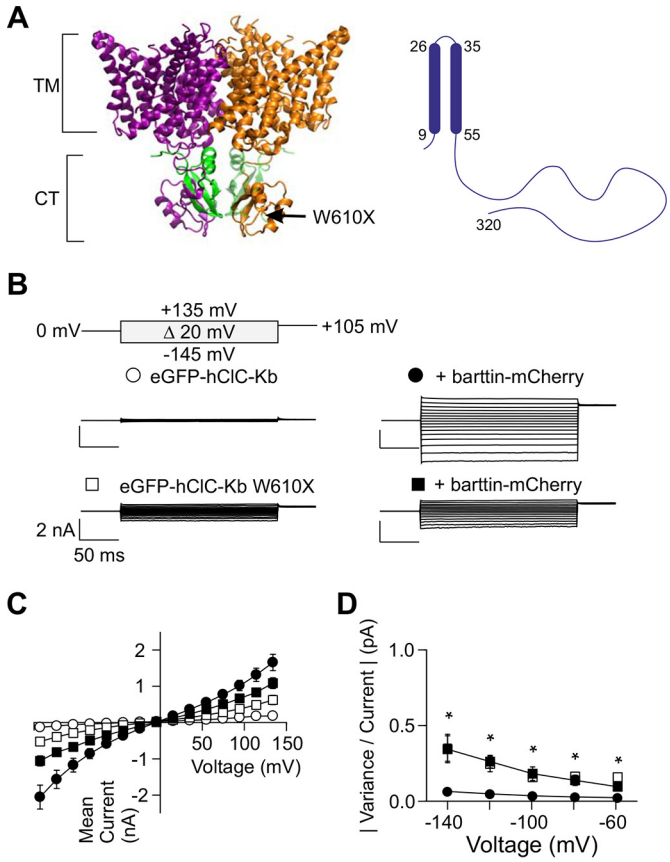

FIGURE 1. **W610X abolishes barttin regulation of hClC-Kb.** *A*, backbone fold of cmClC (3ORG) from the red algae *Cyanidioschyzon merolae* was used for illustration of the transmembrane (TM) and the carboxyl-terminal region (*CT*) as it is the only existing three-dimensional structure encompassing both regions. The two monomers within the dimeric assembly are shown in *purple* and *orange*, respectively. The missing part due to the W610X truncation of the carboxyl terminus in ClC-Kb which includes CBS2 was colored in *green* with the truncation site of the right monomer marked by an *arrow*. The predicted transmembrane topology of barttin is shown on the right side in *blue*. *B*, representative whole-cell current recordings from HEK293T cells expressing full-length or W610X hClC-Kb in the presence or absence of barttin. *C*, current-voltage plots for WT (*open circles* without barttin, n = 10; *filled circles* with barttin, n = 8) and mutant hClC-Kb (*open squares* without barttin, n = 11; *filled squares* with barttin, n = 8). *D*, voltage dependence of the ratio of the current variance by the mean current amplitude for WT with barttin (n = 7) and mutant hClC-Kb with (n = 8; $p < 0.05$ *versus* WT) and without barttin (n = 11; $p < 0.05$ *versus* WT). Student's *t* test was used for statistical comparison.

finding demonstrates a significant change in W610X hClC-Kb channel function.

W610X hClC-Kb/barttin currents were smaller than WT hClC-Kb/barttin currents ($p = 0.03$ at -105 mV; Fig. 1*B*). This difference indicates either reduced W610X hClC-Kb/barttin unitary current amplitudes, reduced absolute open probabilities of W610X hClC-Kb/barttin or smaller numbers of functional W610X hClC-Kb/barttin channels in the surface membrane. We used noise analysis to test for W610X-mediated changes in unitary channel properties. Ion channel currents are usually associated with Lorentzian noise generated by the random opening and closing of individual channels. The current variance (noise) depends on the unitary current amplitude, the absolute open probability and the number of channels. For hClC-Kb the quantitative analysis of current noise is complicated by the double-barreled architecture of this class of channels (3, 37). Each CLC channel exhibits two identical ion conduction pathways (protopores). There are two structurally distinct gating processes, protopore gating that opens and closes individual protopores independently of the adjacent subunit and common gating jointly acting on both pores at once. For such channels, the mean whole-cell current amplitude (I) and the variance σ^2 depend on the number of channels N, the single channel amplitude of an individual protopore i, as well as on the open probabilities of the protopore and the common gate (P_p and P_c) (1, 27, 38):

$$I = 2NiP_pP_c \quad \text{(Eq. 1)}$$

and

$$\sigma^2 = (1 + P_p) \cdot iI - \left(\frac{I^2}{N}\right) \quad \text{(Eq. 2)}$$

Dividing the variance by the mean currents results in:

$$\frac{\sigma^2}{I} = i - iP_p(2P_c - 1) \quad \text{(Eq. 3)}$$

$$= i(1 - P_p(2P_c - 1))$$

To facilitate the understanding and the comparison across different voltage ranges, we only consider the absolute value of this ratio ($|\sigma^2/I|$). Differences in expression levels would leave the ratio unaffected, whereas decreased unitary current amplitudes would cause lower values of $|\sigma^2/I|$. In contrast, decreased absolute open probabilities will augment this ratio. We found that ratios of current variances by the mean currents over a stable segment of our current recordings were larger for W610X than for WT eGFP-hClC-Kb/barttin (Fig. 1*D*; $p < 0.05$ for all voltages shown). This result indicates that the W610X mutation decreased absolute open probabilities of hClC-Kb/barttin channels. Furthermore, we observed identical $|\sigma^2/I|$ values for cells co-expressing W610X hClC-Kb with barttin and for cells that exclusively express the truncated channel, indicating that barttin failed to modify unitary properties of truncated hClC-Kb channels (Fig. 1*D*).

Barttin Increases Expression Levels of WT and W610X hClC-Kb—Barttin increases WT CLC-K expression levels by impairing degradation of the channel protein (39, 40). The difference in whole-cell current amplitudes between cells expressing W610X eGFP-hClC-Kb alone or together with barttin (Fig. 1*C*) might therefore be due to increased mutant channel expression in the presence of the accessory subunit. We expressed WT and mutant eGFP-hClC-Kb alone or together with barttin in HEK293T cells and resolved the fluorescent fusion proteins by SDS-PAGE (Fig. 2*A*). Fluorescence intensities demonstrated higher expression levels of WT and W610X eGFP-hClC-Kb in the presence than in the absence of barttin. To quantify the effects of barttin on hClC-Kb protein expression, we calculated the ratios of expression levels with barttin relative to the levels without barttin (Fig. 2*B*). This analysis revealed a barttin-dependent increase of WT eGFP-hClC-Kb expression by 3.44 ± 0.96 ($n = 6$) and of 1.81 ± 0.10 ($n = 8$) for W610X eGFP-hClC-Kb. We conclude that the preventive effect of barttin on channel degradation is preserved for truncated hClC-Kb. Enhanced expression of W610X hClC-Kb explains the larger current amplitudes in cells co-expressing barttin (Fig. 1*C*), although the functional properties of individual channels are not altered by the accessory subunit (Fig. 1*C*).

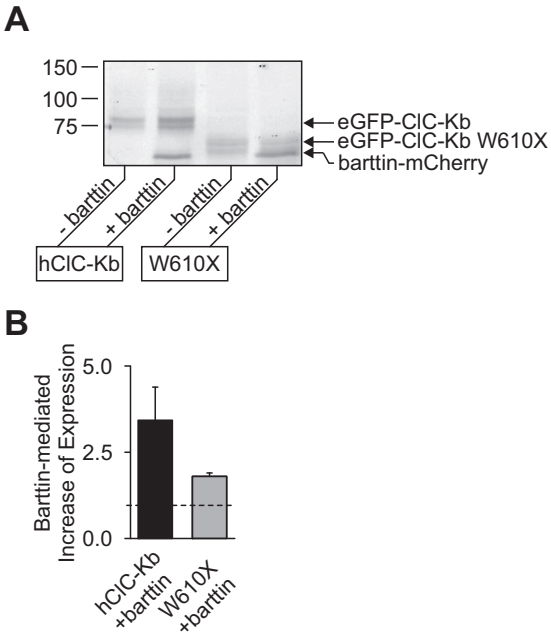

FIGURE 2. **Barttin increases the number of WT and mutant hClC-Kb proteins in transfected cells.** *A*, representative eGFP and mCherry fluorescence scan of an SDS-PAGE of lysates from HEK293T cells expressing WT or W610X eGFP-hClC-Kb in the presence or absence of barttin-mCherry. *B*, ratios of expression levels of full-length ($n = 6$) or truncated hClC-Kb ($n = 8$) in the presence of barttin by the corresponding values in the absence of barttin.

Carboxyl-terminal Truncations Do Not Impair Association with Barttin—We next quantified the association of barttin with WT or mutant hClC-Kb by co-transfecting HEK293T cells with barttin-mYFP and either full-length or truncated mCherry-hClC-Kb. For each experiment, the cleared lysates were divided in two equal portions after solubilization of channel complexes with detergent. One was incubated with an anti-GFP antibody, and protein G-coupled agarose beads were then used to purify barttin-mYFP and associated proteins from the lysate (Fig. 3*A*). Using this procedure we co-purified similar fractions of mCherry-hClC-Kb (0.58 ± 0.07, $n = 3$) or W610X

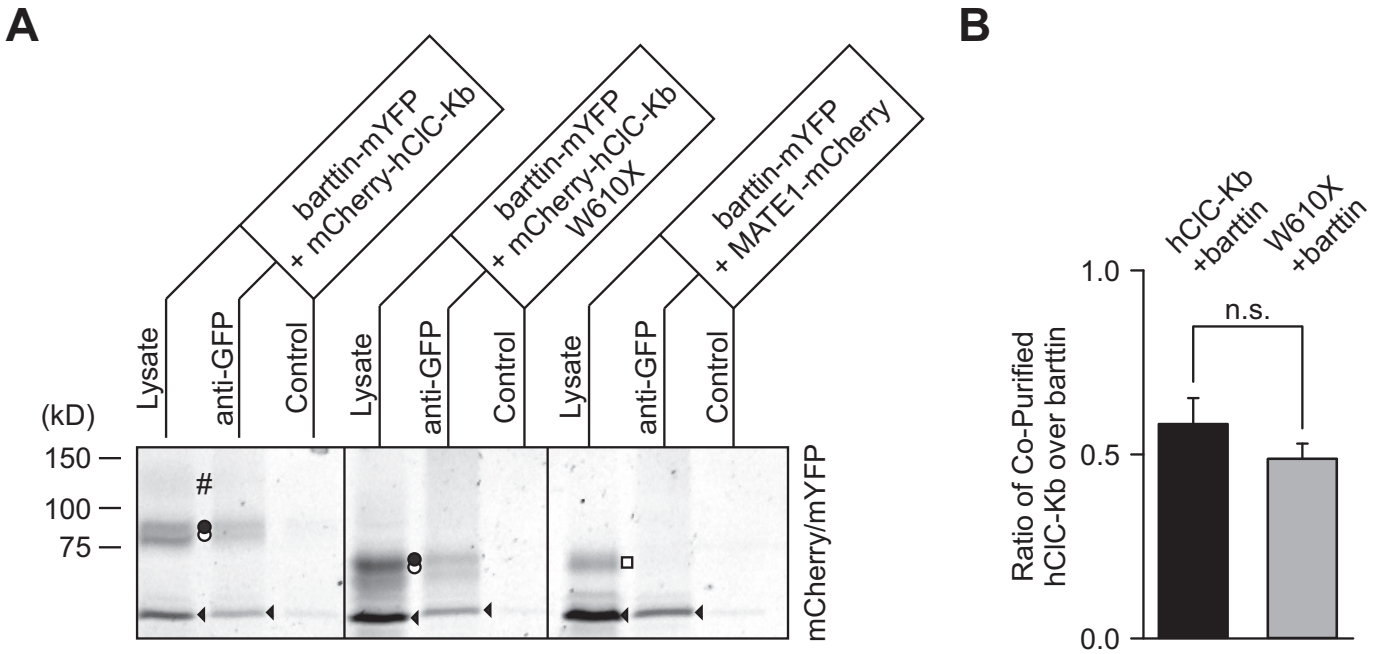

FIGURE 3. **W610X does not impair hClC-Kb association with barttin.** *A*, combined eGFP and mCherry fluorescence scan of a representative 10% SDS gel. Signals can be observed in lanes loaded with sample incubated with anti-GFP antibody and the lysate, but not in the control lane, which was not incubated with the antibody. WT and W610X mCherry-hClC-Kb exist as non-glycosylated (*open circle*) and core-glycosylated proteins (*filled circle*). Complex-glycosylation (#) of hClC-Kb is much more pronounced for WT than for W610X. MATE-1 mCherry (*open square*), which is not known to bind to barttin, was used as a negative control. *B*, ratios of eluted mCherry-hClC-Kb or mCherry-hClC-Kb W610X over the barttin-mYFP fluorescence amplitudes ($n = 3$ each; "n.s." indicates $p = 0.31$ using Student's *t* test).

mCherry-hClC-Kb (0.49 ± 0.04, $n = 3$, $p = 0.31$; Fig. 3*B*). To test the specificity of our approach, we left the other lysate portion as control without antibody for each experiment, but treated it identically in all other respects. Almost no signals were obtained from these samples indicating only a low degree of unspecific association of hClC-Kb/barttin with the agarose used in the purification procedure.

Barttin appears to interact via multiple hydrophobic residues with CLC-K (28, 41), and such interactions might produce unspecific binding events in co-immunoprecipitation experiments. We therefore performed control experiments with a member of an unrelated family of membrane proteins, the multidrug and toxin extrusion proteins (MATE). Cells were co-transfected with barttin-mYFP and MATE1-mCherry (42). Although MATE1 expresses well in HEK293T cells, as indicated by the prominent fluorescent band in the cleared lysate, no protein could be purified using the anti-GFP antibody (Fig. 3*A*). Another unrelated anion exchanger, SLC26A9-mCherry (43), could also not be co-purified with barttin-mYFP (data not shown). We conclude from these experiments that W610X does not prevent the association of hClC-Kb and barttin.

W610X Impairs Surface Membrane Insertion of hClC-Kb/Barttin—We next studied the subcellular distribution of fluorescent fusion proteins of WT and W610X hClC-Kb and barttin using confocal microscopy on transfected MDCKII cells. When expressed alone, eGFP-hClC-Kb predominantly localizes to the endoplasmic reticulum, in agreement with earlier results (6) (Fig. 4*A*). Transient transfection with barttin-mCherry alone resulted in a strong membrane staining (Fig. 4*B*). Co-transfection of hClC-Kb with barttin promoted surface membrane insertion of the channel (26), resulting in overlapping membrane staining by eGFP-hClC-Kb and barttin-mCherry (Fig. 4*C*).

The distribution of W610X eGFP-hClC-Kb in the presence of barttin closely resembled the distribution of WT hClC-Kb in the absence of barttin (Fig. 4*D*). Although barttin still exhibited some degree of plasma membrane-like staining in these cells, most of the mCherry signal was retained intracellularly (Fig. 4*D*). Co-staining with Calnexin, a marker for the endoplasmic reticulum, confirmed that the intracellular staining for hClC-Kb W610X/barttin was mostly confined to the ER as observed for the wild type without barttin (data not shown). These findings support the notion that W610X results in intracellular retention of hClC-Kb/barttin complexes.

We next employed surface biotinylation to quantify the effects of W610X on hClC-Kb/barttin trafficking. Channels inserted into the surface membrane of living MDCK II cells were labeled using a hydrophilic reactive biotin derivative, lysed, and then purified using streptavidin-coated agarose beads. The use of the amino-terminally eGFP-labeled constructs allowed the determination of expression levels and relative surface insertion by fluorescence scanning of SDS-PAGE gels (Fig. 4*E*). We quantified the amount of WT and mutant hClC-Kb in the whole cell lysate and the eluate from streptavidin-coated beads. The surface membrane fractions were then determined as ratio of these two signals.

Fig. 4*F* shows mean values of the surface membrane fractions from cells expressing WT or W610X hClC-Kb, either expressed alone or together with barttin. For each experiment the ratios were normalized to the value obtained with WT hClC-Kb co-expressed with barttin in the same series of experiments. As already shown in previous publications, WT hClC-Kb resides in

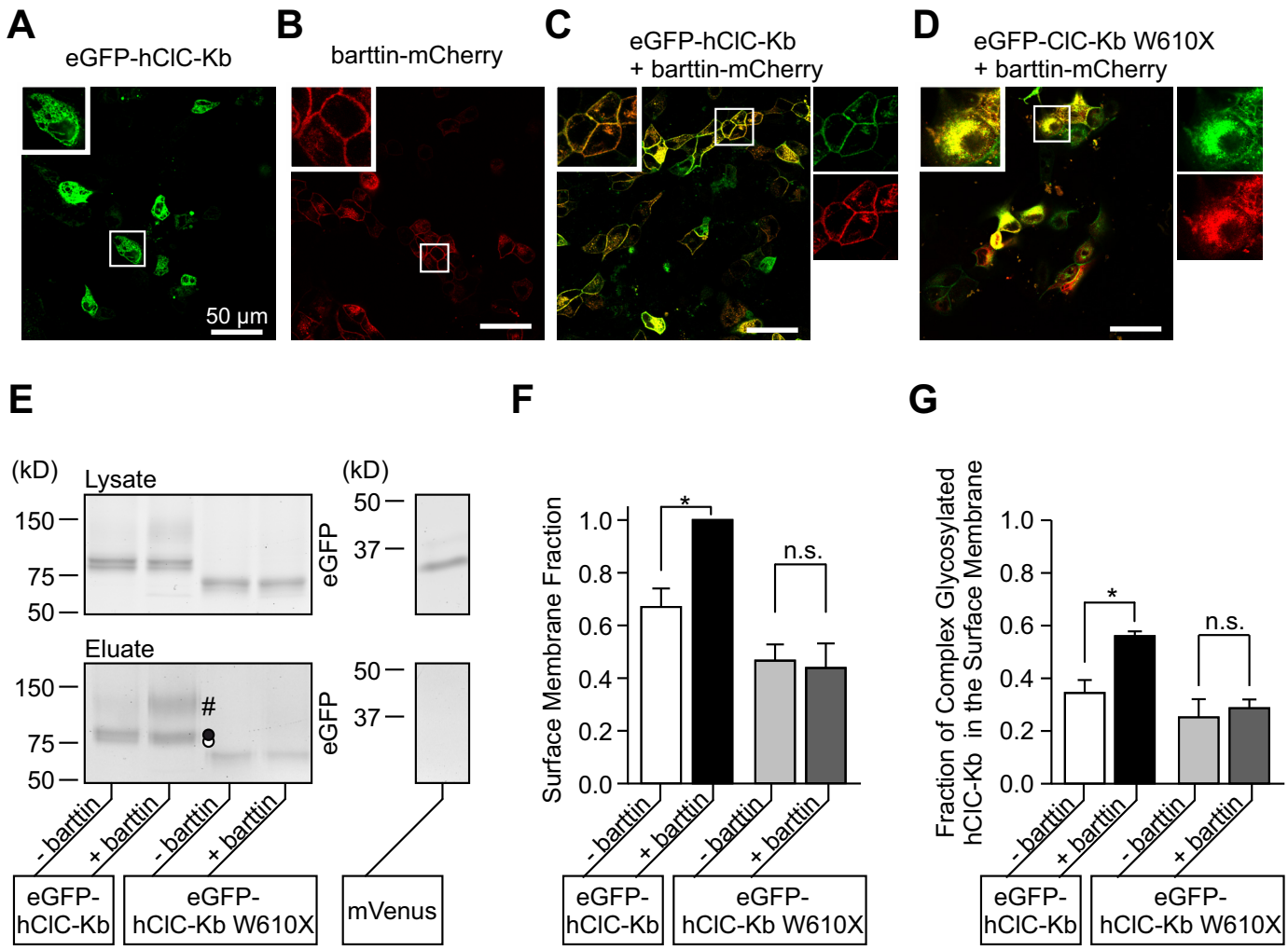

FIGURE 4. **W610X hClC-Kb/barttin is retained in intracellular cell compartments.** *A–D*, representative confocal images of cells expressing barttin-mCherry or WT eGFP-hClC-Kb alone, as well as WT or W610X eGFP-hClC-Kb together with barttin as indicated. eGFP was fused to the amino terminus of hClC-Kb (*green*) and mCherry to the carboxyl terminus of barttin (*red*). Regions in which pore-forming and accessory subunits overlap are colored in *yellow*. *E*, eGFP/mVenus fluorescence scans of representative SDS-PAGE of lysate and eluate fractions from biotinylation experiments on cells expressing eGFP-hClC-Kb or W610X eGFP-hClC-Kb with or without barttin. The channels exist in a complex-glycosylated (#), a core-glycosylated (*filled circle*) and in a non-glycosylated state (*open circle*). A representative control experiment on cells expressing the soluble mVenus protein illustrates lack of mVenus in the eluate indicating that cytosolic proteins are not biotinylated. *F*, surface membrane insertion probability was calculated as the ratio of the total intensity (all glycosylation states) in the eluate fraction by the total intensity in the lysate ($n = 5$ for all samples; * indicates $p = 0.008$; "n.s." indicates $p = 0.81$; Student's *t* test was used for comparison). *G*, fraction of complex glycosylated proteins reveals no enhancement of glycosylation for truncated hClC-Kb channels upon co-expression of barttin ($n = 5$ for all samples except W610X without barttin: $n = 4$; * indicates $p = 0.003$; "n.s." indicates = 0.35; Student's *t* test was used for comparison).

the plasma membrane in significant amounts even in the absence of barttin (*white bar*, 0.67 ± 0.07, $n = 5$), and co-expression of barttin increases surface membrane insertion only by 50%. W610X hClC-Kb alone exhibits slightly lower surface insertion levels that, unlike for WT hClC-Kb, cannot be enhanced by the co-expression of barttin (*light gray bar*, without barttin: 0.47 ± 0.06; *dark gray bar*, with barttin: 0.44 ± 0.09, $n = 5$ each).

To test whether intracellular ClC-Kb might also be biotinylated using our protocol, for example from damaged cells, we used cells transfected with the cytosolic protein mVenus as control. The sole occurrence of mVenus in the lysate, but not in the eluate (Fig. 4*E*) verifies that only proteins exposed in the surface membrane were biotinylated in our experiments.

CLC-K channels migrate in three different bands on reducing SDS-PAGE that were shown to represent non- (*open circles*), core- (*filled circles*) and complex-glycosylated protein (#) (Figs. 3*A* and 4*E*) (26, 44). Complex glycosylation of hClC-Kb differs significantly for channels expressed together or without barttin (26). In the absence of barttin, WT hClC-Kb exhibits a basal level of complex glycosylation in the surface membrane fraction as determined by the ratio of the intensity of the band representing complex-glycosylated protein (#) to the sum of all three bands (Fig. 4*G*; *white bar*, 0.34 ± 0.05, $n = 5$) that is significantly increased in cells co-expressing barttin (*black bar*, 0.56 ± 0.02, $n = 5$; $p = 0.003$). Whereas W610X hClC-Kb displays a similar level of complex glycosylation as full-length hClC-Kb (*light gray bar*, 0.25 ± 0.07, $n = 4$; $p = 0.30$) in the absence of barttin, the subunit fails to promote complex glycosylation of the mutant channel (*dark gray bar*, 0.35 ± 0.05, $n = 5$; $p = 0.35$ *versus* hClC-Kb W610X alone).

Carboxyl-terminal Truncations of rClC-K1 Channels Result in Channel Gating that Is Not Modified by Barttin—rClC-K1 is the rat homolog of hClC-Ka. It is 80% identical to its human

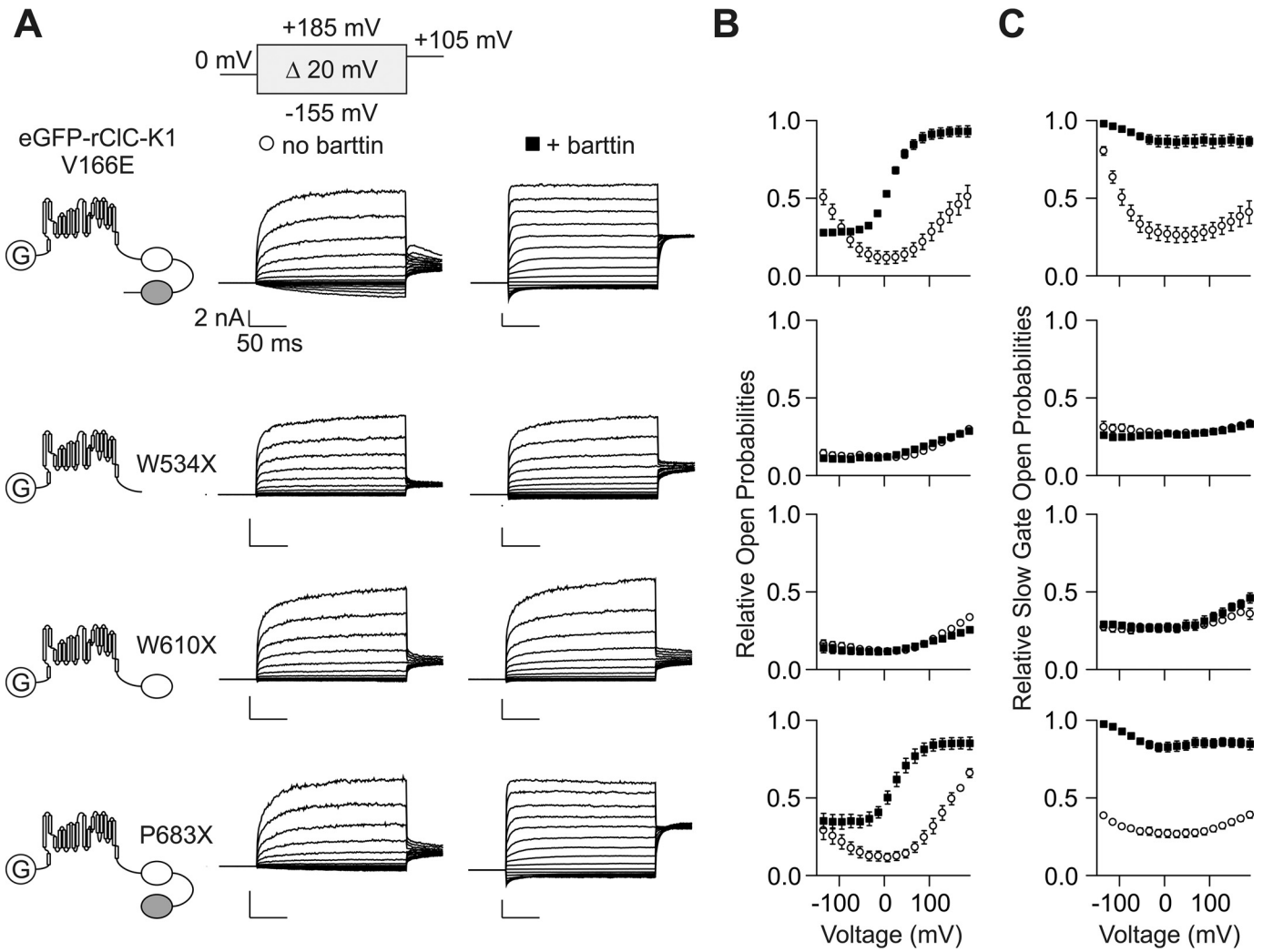

FIGURE 5. **The second CBS domain is required for gating modification of V166E rClC-K1 by barttin.** *A*, representative recordings from cells expressing WT, W534X, W610X, or P683X V166E eGFP-rClC-K1 alone (*middle column*) or together with barttin-mCherry (*right column*). Transmembrane topology models illustrate the degrees of carboxyl-terminal truncations in the tested channel proteins (GFP: *white circle* marked with "G"; CBS1: *white oval*; CBS2: *gray oval*). *B*, voltage dependence of relative open probabilities of WT and truncated V166E rClC-K1 either expressed alone (*open symbol*; $n = 8–12$) or with barttin (*closed symbol*; $n = 5–14$). Values in the absence of barttin were normalized to the lowest value of V166E rClC-K1 in the absence of barttin. *C*, slow gate open probabilities were obtained by dividing instantaneous current amplitudes after a 15 ms pulse to +185 mV that fully activates the protopore gates by corresponding amplitudes without this activating pulse ($n = 4–9$).

counterpart and shows similar localization and cellular functions (4). However, in contrast to hClC-Ka and hClC-Kb, rClC-K1 can form functional channels also in the absence of barttin (4, 6, 7). This property permits studying the effects of barttin on rClC-K1 gating and allowed identification of mechanisms underlying the functional CLC-K modification by barttin (27, 45). We decided to use rClC-K1 carrying the V166E mutation to characterize the effects of carboxyl-terminal truncations on CLC-K function. The V166E mutation introduces the so-called "gating glutamate" that is conserved in all mammalian CLC proteins except for CLC-K channels (6). This mutation endows rClC-K1 with pronounced barttin-dependent changes in time- and voltage dependence (Fig. 5, *A–C*) (6, 27).

We combined the V166E mutation with three different truncations, one deleting almost the complete carboxyl terminus (W534X), another one corresponding to the naturally occurring mutation of hClC-Kb (W610X) and a third one (P683X) that only deletes the last five amino-acids of the channel immediately succeeding the second CBS domain (Fig. 5*A*). Full-length as well as all truncated V166E eGFP-rClC-K1 exhibited activation at positive voltages in the absence of barttin. In contrast, we observed the characteristic slow activation by voltages below the reversal potential for chloride only in full-length channels (Fig. 5*A*). P683X/V166E eGFP-rClC-K1 exhibited slight hyperpolarization-induced activation that was altogether absent in W610X/V166E and W534X/V166E eGFP-rClC-K1. Co-expression of V166E eGFP-rClC-K1 and barttin increased the macroscopic current amplitudes, accelerated activation at positive and resulted in deactivation at negative potentials (Fig. 5*A*, *top*). Barttin-modified P683X/V166E eGFP-rClC-K1 channels in a similar way (Fig. 5*A*, *bottom*), however, failed to modify the W534X and W610X truncations (Fig. 5*A*, *middle*). Separating the slow gate open probabilities by inserting a short activating step previous to the test pulse to +105 mV, which opens the fast gate to a fixed value (27) revealed barttin-mediated changes

in slow gate activation for V166E and P683X/V166E eGFP-rClC-K1, but not for the other truncated channels (Fig. 5*C*).

In the absence of barttin, P683X/V166E eGFP-rClC-K1 channels showed an attenuation of the characteristic slow gate activation at negative voltages (Fig. 5, *B* and *C*). We conclude that the last five amino acids contribute to slow common gating in the absence, but not in the presence of barttin. Taken together, these results suggest that the second CBS domain is essential for the effect of barttin on common gating.

Discussion

All mammalian CLCs exhibit cytoplasmic carboxyl termini with two so-called cystathionine-β-synthase (CBS) domains. The CBS domains themselves are generally well conserved, whereas the unstructured regions comprising the rest of the carboxyl terminus significantly differ in length and amino acid composition between distinct CLC isoforms (46). We here performed a detailed analysis of the functional consequences of a naturally occurring mutation of hClC-Kb that is frequently found in patients with Bartter syndrome type III. We demonstrate that the loss of CBS2 in the carboxyl terminus of hClC-Kb (W610X) abolishes channel regulation by barttin. W610X hClC-Kb is functional in the absence of barttin and not further activated by co-expression of the accessory subunit (Fig. 1). Moreover, barttin fails to modify W610X hClC-Kb trafficking as well as its complex glycosylation (Fig. 4).

The intracellular carboxyl termini of CLC channels and transporters might interact with intracellular signal cascades and thus permit adjustment of chloride transport by regulatory pathways. The role of the CLC carboxyl terminus was first studied in a CLC channel from the electric organ of *Torpedo marmorata* (ClC-0). Expression of truncated ClC-0 channels revealed that intact carboxyl termini are necessary for anion currents in *Xenopus* oocytes and that the co-expression of complementary sequences sometimes restores functional expression (47). In this initial study effects on channel function and trafficking were not distinguished. Later work demonstrated that CBS domains are important for normal function of the muscle chloride channel hClC-1 and the ubiquitously expressed hClC-2 channel (48–51). hClC-1 only tolerated truncations distal to the second CBS domain, and deletion of additional protein regions resulted in loss-of-function (48). In this study, the effects on the subcellular distribution were only studied by confocal imaging, and none of the truncated hClC-1 exhibited major changes on this parameter (48). For hClC-2, ATP binding to the CBS domains results in longer slow gate closures (51), and removal of the full carboxyl terminus accelerates hClC-2 gating by preventing slow gate closures (50). Multiple partial carboxyl-terminal truncations and deletions constitutively locked hClC-2 in a closed conformation, without any effect on surface membrane insertion (50). For CLC anion/proton antiporters that normally reside in intracellular cell organelles crucial roles for correct trafficking and sorting have been assigned to the carboxyl terminus (52–55). The chloride/proton antiporter hClC-7 is the only other member of the CLC family with an obligatory subunit, Ostm1, which is needed for proper function and subcellular localization (56). Several disease-causing mutations in the CBS2 region of hClC-7 interfere with normal gating of this transporter in the presence of its subunit (57).

A significant fraction of WT hClC-Kb channels insert into the plasma membrane of HEK293T and MDCK II cells even in the absence of barttin (6, 26, 28) (Fig. 4*F*). Whereas barttin increases the number of WT hClC-Kb in the surface membrane, we neither observed any barttin-dependent modification of the subcellular distribution of W610X hClC-Kb in confocal images nor in surface biotinylation experiments (Fig. 4). W610X hClC-Kb channels additionally showed reduced complex glycosylation (Fig. 4*G*). Since this post-translational modification occurs during protein passage through the Golgi apparatus, its reduction in W610X hClC-Kb channels indicates that truncated channels are not subject to the normal trafficking. Although W610X channels are constitutively active, they show a reduced and barttin-independent absolute open probability (Fig. 1).

This retention of W610X hClC-Kb in the endoplasmic reticulum predicts a significant reduction of the baso-lateral chloride conductance in the thick ascending limb of Henle. Although we cannot rule out a differential effect of mutant hClC-Kb in human kidney cells, the MDCK II cell system represents an established model for studying protein trafficking in epithelial cells (58). The reduction in membrane insertion and the reduction of the absolute chloride conductance seem to be a common hallmark of Bartter syndrome associated mutations in hClC-Kb (59, 64). Furthermore, the symptoms of affected individuals can be appropriately explained by a reduction in the baso-lateral chloride conductance of the thick ascending limb which leads to an increase in the intracellular chloride concentration which in turn reduces the uptake of sodium, chloride and potassium by the Na^+-K^+-$2Cl^-$ symporter NKCC2. This lack of sodium chloride reabsorption also limits water transport and thus urinary concentration. The small constitutive current of W610X hClC-Kb is obviously not sufficient to keep-up with the needed reabsorption of chloride.

Barttin appears to bind to ClC-K via multiple hydrophobic interactions between the first transmembrane helix of barttin (28) and helices B and/or J (41). In agreement with this notion W610X does not affect hClC-Kb/barttin function via impaired barttin-hClC-Kb association. Co-immunoprecipitation experiments (Fig. 3) demonstrated that similar amounts of barttin can be co-purified with WT and W610X hClC-Kb, in agreement with earlier reports on truncated rat ClC-K2 channels which retained the ability for association with barttin (39). Confocal imaging demonstrated that MDCK cells expressing barttin alone or together with WT hClC-Kb exhibit prominent plasma membrane staining of the subunit. In contrast, W610X hClC-Kb and barttin co-localize in the endoplasmic reticulum (Fig. 4, *A–D*), indicating association of the accessory subunit with the trafficking-impaired W610X hClC-Kb. Moreover, barttin increases expression levels of WT as well as of W610X hClC-Kb (Fig. 2). We thus conclude that the W610X hClC-Kb/barttin complexes assemble normally, but fail to leave the endoplasmic reticulum and to insert properly into the surface membrane.

Whereas barttin only increases the fraction of surface membrane-inserted CLC-K channels by about 50% (Fig. 3), it is

essential for the function of human CLC-K channels. hClC-Ka and hClC-Kb are non-functional when expressed alone and require barttin to become functional anion channels. This switch is likely mediated by the modification of channel gating (27). The rodent CLC-K isoform rClC-K1 is active also in the absence of barttin and exhibits fast protopore and slow common gating steps. Co-expression of rClC-K1 and barttin results in a permanently open common gate (27, 45). Although such effect on the common gate of human CLC-K channel function cannot be directly demonstrated, we recently demonstrated that hClC-Ka/barttin channels exhibit an open common gate (27). Moreover, scanning mutagenesis demonstrated similar effects of tryptophan insertion at each transmembrane domain of barttin on common gating of rClC-K1 and function of hClC-Ka (28). Taken together, these findings strongly suggest that barttin activates human and rodent CLC-K by the same mechanisms, *i.e.* by opening the common gate.

We therefore employed the V166E rClC-K1 system to elucidate the effects of carboxyl-terminal truncations on CLC-K gating. Mutant V166E rClC-K1, truncated either at Trp-610 or lacking the whole carboxyl terminus (W534X) did not exhibit the characteristic slow gating of full-length channels in the absence of barttin (Fig. 4*B*) and were not activated by barttin (Fig. 4*C*). These data provide a possible mechanism by which W610X might alter the barttin-induced modification of hClC-Kb function. WT hClC-Kb is closed by the common gate in the absence of barttin, and assembly with the accessory subunit results in its opening. W610X results in partial, barttin-independent common gate opening, thus resulting in currents in the absence of barttin, but lacking current stimulation by barttin. Removal of five amino acids (PPAPK) immediately after the second CBS domain result in less pronounced slow gating in the absence of barttin and in currents similar to WT hClC-Kb in the presence of barttin. These results suggest that the PPAPK sequence motif might modify opening of the common gate.

Human barttin consists of 320 amino acids, but the first 71 amino acids are sufficient for channel activation (6). This essential barttin portion contains the two predicted transmembrane helices (8) that are necessary for association of subunit and channel (28, 60), the cytosolic amino terminus and 18 amino acids carboxyl-terminal to TM2. Several disease-causing mutations in the cytosolic amino terminus of barttin lack activation of CLC-K channels upon co-expression (26). Recently, it was shown that cysteines at positions 54 and 56, located immediately after the second transmembrane domain of barttin, must be palmitoylated for the activation of CLC-K channels (29). These findings might support a possible interaction of the CBS2 domain of ClC-Kb with the cytosolic amino acids close to the transmembrane core (61). Since the activity of human CLC-K channels is tightly linked to the presence and function of barttin, one might imagine that dynamic changes of palmitoylation play a role in the adjustment of chloride conductances in the loop of Henle. This regulation of barttin would be impossible in truncated hClC-Kb channels.

The fact that carboxyl-terminal truncations of ClC-Kb do not lead to a complete loss-of-function might warrant further studies into pharmacological interventions. There are reports that certain fenamates activate ClC-Kb in *Xenopus laevis* oocytes (62) but not in mammalian cell systems such as HEK293 or MDCK II (31). Another approach might be to increase the exit of W610X from the endoplasmic reticulum. For the barttin mutants R8L and G47R, plasma membrane insertion and hearing thresholds in knock-in mice could be increased by an Hsp90 inhibitor (63). However, it remains unclear whether this approach also affects ER exit of ClC-Kb channels.

In conclusion, we here demonstrate that the second CBS domain is important for proper exit of the hClC-Kb/barttin complex from the endoplasmic reticulum through the Golgi apparatus to the plasma membrane. The loss of the second CBS domain results in fewer channels in the plasma membrane. Although these channels are active, this remaining W610X hClC-Kb function is insufficient for proper renal function. Any truncation of hClC-Kb found proximal to the second CBS domain should therefore be considered as loss of function mutation causing Bartter syndrome type III.

Author Contributions—G. S. and Ch. F. designed the study and wrote the paper. G. S. performed patch clamp, confocal microscopy, and co-immunoprecipitation experiments. G. S. and S. B-P. performed and analyzed surface biotinylation experiments. G. S. and A. F. designed and constructed the plasmids used. All authors approved the final version of the manuscript.

Acknowledgments—Expression constructs for barttin, hClC-Kb, and rClC-K1 were kindly provided by Drs. A. L. George and S. Uchida. We thank Drs. Martin Fischer, Raul Guzman, and Daniel Wojciechowski for helpful discussions.

References

1. Stölting, G., Fischer, M., and Fahlke, C. (2014) CLC channel function and dysfunction in health and disease. *Front Physiol.* **5,** 378
2. Miller, C., and White, M. M. (1984) Dimeric structure of single chloride channels from Torpedo electroplax. *Proc. Natl. Acad. Sci. U.S.A.* **81,** 2772–2775
3. Dutzler, R., Campbell, E. B., Cadene, M., Chait, B. T., and MacKinnon, R. (2002) X-ray structure of a ClC chloride channel at 3.0 A reveals the molecular basis of anion selectivity. *Nature* **415,** 287–294
4. Uchida, S., Sasaki, S., Nitta, K., Uchida, K., Horita, S., Nihei, H., and Marumo, F. (1995) Localization and functional characterization of rat kidney-specific chloride channel, ClC-K1. *J. Clin. Invest.* **95,** 104–113
5. Vandewalle, A., Cluzeaud, F., Bens, M., Kieferle, S., Steinmeyer, K., and Jentsch, T. J. (1997) Localization and induction by dehydration of ClC-K chloride channels in the rat kidney. *Am. J. Physiol.* **272,** F678–688
6. Scholl, U., Hebeisen, S., Janssen, A. G. H., Müller-Newen, G., Alekov, A., and Fahlke, C. (2006) Barttin modulates trafficking and function of ClC-K channels. *Proc. Natl. Acad. Sci. U.S.A.* **103,** 11411–11416
7. Waldegger, S., Jeck, N., Barth, P., Peters, M., Vitzthum, H., Wolf, K., Kurtz, A., Konrad, M., and Seyberth, H. W. (2014) Barttin increases surface expression and changes current properties of ClC-K channels. *Pflugers Arch.* **444,** 411–418
8. Estévez, R., Boettger, T., Stein, V., Birkenhäger, R., Otto, E., Hildebrandt, F., and Jentsch, T. J. (2001) Barttin is a Cl^- channel beta-subunit crucial for renal Cl^- reabsorption and inner ear K^+ secretion. *Nature* **414,** 558–561
9. Fahlke, C., and Fischer, M. (2010) Physiology and pathophysiology of ClC-K/barttin channels. *Front. Physiol.* **1,** 155
10. Barlassina, C., Dal Fiume, C., Lanzani, C., Manunta, P., Guffanti, G., Ruello, A., Bianchi, G., Del Vecchio, L., Macciardi, F., and Cusi, D. (2007) Common genetic variants and haplotypes in renal *CLCNKA* gene are associated to salt-sensitive hypertension. *Hum. Mol. Genet.* **16,** 1630–1638

11. Cappola, T. P., Matkovich, S. J., Wang, W., van Booven, D., Li, M., Wang, X., Qu, L., Sweitzer, N. K., Fang, J. C., Reilly, M. P., Hakonarson, H., Nerbonne, J. M., and Dorn, G. W., 2nd. (2011) Loss-of-function DNA sequence variant in the *CLCNKA* chloride channel implicates the cardio-renal axis in interindividual heart failure risk variation. *Proc. Natl. Acad. Sci.* **108,** 2456–2461
12. Bartter, F. C., Pronove, P., Gill Jr., J. R., and MacCardle, R. C. (1962) Hyperplasia of the juxtaglomerular complex with hyperaldosteronism and hypokalemic alkalosis: A new syndrome. *Am. J. Med.* **33,** 811–828
13. Simon, D. B., Bindra, R. S., Mansfield, T. A., Nelson-Williams, C., Mendonca, E., Stone, R., Schurman, S., Nayir, A., Alpay, H., Bakkaloglu, A., Rodriguez-Soriano, J., Morales, J. M., Sanjad, S. A., Taylor, C. M., Pilz, D., Brem, A., Trachtman, H., Griswold, W., Richard, G. A., John, E., and Lifton, R. P. (1997) Mutations in the chloride channel gene, *CLCNKB*, cause Bartter's syndrome type III. *Nat. Genet.* **17,** 171–178
14. Hebert, S. C. (2003) Bartter syndrome. *Curr. Opin. Nephrol. Hypertens.* **12,** 527–532
15. Simon, D. B., Karet, F. E., Hamdan, J. M., DiPietro, A., Sanjad, S. A., and Lifton, R. P. (1996) Bartter's syndrome, hypokalaemic alkalosis with hypercalciuria, is caused by mutations in the Na–K–2CI cotransporter NKCC2. *Nat. Genet.* **13,** 183–188
16. Simon, D. B., Karet, F. E., Rodriguez-Soriano, J., Hamdan, J. H., DiPietro, A., Trachtman, H., Sanjad, S. A., and Lifton, R. P. (1996) Genetic heterogeneity of Barter's syndrome revealed by mutations in the K^+ channel, ROMK. *Nat. Genet.* **14,** 152–156
17. Birkenhäger, R., Otto, E., Schürmann, M. J., Vollmer, M., Ruf, E. M., Maier-Lutz, I., Beekmann, F., Fekete, A., Omran, H., Feldmann, D., Milford, D. V., Jeck, N., Konrad, M., Landau, D., Knoers, N. V., Antignac, C., Sudbrak, R., Kispert, A., and Hildebrandt, F. (2001) Mutation of *BSND* causes Bartter syndrome with sensorineural deafness and kidney failure. *Nat. Genet.* **29,** 310–314
18. Vargas-Poussou, R., Huang, C., Hulin, P., Houillier, P., Jeunemaître, X., Paillard, M., Planelles, G., Déchaux, M., Miller, R. T., and Antignac, C. (2002) Functional characterization of a calcium-sensing receptor mutation in severe autosomal dominant hypocalcemia with a Bartter-like syndrome. *J. Am. Soc. Nephrol.* **13,** 2259–2266
19. Watanabe, S., Fukumoto, S., Chang, H., Takeuchi, Y., Hasegawa, Y., Okazaki, R., Chikatsu, N., and Fujita, T. (2002) Association between activating mutations of calcium-sensing receptor and Bartter's syndrome. *Lancet* **360,** 692–694
20. Bettinelli, A., Borsa, N., Bellantuono, R., Syrèn, M.-L., Calabrese, R., Edefonti, A., Komninos, J., Santostefano, M., Beccaria, L., Pela, I., Bianchetti, M. G., and Tedeschi, S. (2007) Patients with biallelic mutations in the chloride channel gene *CLCNKB*: long-term management and outcome. *Am. J. Kidney Dis.* **49,** 91–98
21. Velázquez, H., and Silva, T. (2003) Cloning and localization of KCC4 in rabbit kidney: expression in distal convoluted tubule. *Am. J. Physiol. Renal Physiol.* **285,** F49-F58
22. Andrini, O., Keck, M., Briones, R., Lourdel, S., Vargas-Poussou, R., and Teulon, J. (2015) ClC-K chloride channels: Emerging pathophysiology of Bartter syndrome type 3. *Am. J. Physiol. Renal Physiol.* 10.1152/ajprenal.00004.2015
23. Fukuyama, S., Hiramatsu, M., Akagi, M., Higa, M., and Ohta, T. (2004) Novel mutations of the chloride channel Kb gene in two Japanese patients clinically diagnosed as Bartter syndrome with hypocalciuria. *J. Clin. Endocrinol. Metab.* **89,** 5847–5850
24. Nozu, K., Iijima, K., Kanda, K., Nakanishi, K., Yoshikawa, N., Satomura, K., Kaito, H., Hashimura, Y., Ninchoji, T., Komatsu, H., Kamei, K., Miyashita, R., Kugo, M., Ohashi, H., Yamazaki, H., Mabe, H., Otsubo, A., Igarashi, T., and Matsuo, M. (2010) The pharmacological characteristics of molecular-based inherited salt-losing tubulopathies. *J. Clin. Endocrinol. Metab.* **95,** E511–E518
25. Lee, B. H., Cho, H. Y., Lee, H., Han, K. H., Kang, H. G., Ha, I. S., Lee, J. H., Park, Y. S., Shin, J. I., Lee, D.-Y., Kim, S.-Y., Choi, Y., and Cheong, H. I. (2012) Genetic basis of Bartter syndrome in Korea. *Nephrol. Dial. Transplant.* **27,** 1516–1521
26. Janssen, A. G. H., Scholl, U., Domeyer, C., Nothmann, D., Leinenweber, A., and Fahlke, C. (2009) Disease-causing dysfunctions of Barttin in Bartter syndrome type IV. *J. Am. Soc. Nephrol.* **20,** 145–153
27. Fischer, M., Janssen, A. G. H., and Fahlke, C. (2010) Barttin activates ClC-K channel function by modulating gating. *J. Am. Soc. Nephrol.* **21,** 1281–1289
28. Wojciechowski, D., Fischer, M., and Fahlke, C. (2015) Tryptophan scanning mutagenesis identifies the molecular determinants of distinct Barttin functions. *J. Biol. Chem.* **290,** 18732–18743
29. Steinke, K. V., Gorinski, N., Wojciechowski, D., Todorov, V., Guseva, D., Ponimaskin, E., Fahlke, C., and Fischer, M. (2015) Human CLC-K channels require palmitoylation of their accessory subunit Barttin to be functional. *J. Biol. Chem.* **290,** 17390–17400
30. Ho, S. N., Hunt, H. D., Horton, R. M., Pullen, J. K., and Pease, L. R. (1989) Site-directed mutagenesis by overlap extension using the polymerase chain reaction. *Gene.* **77,** 51–59
31. Imbrici, P., Liantonio, A., Gradogna, A., Pusch, M., and Camerino, D. C. (2014) Targeting kidney CLC-K channels: pharmacological profile in a human cell line versus Xenopus oocytes. *Biochim. Biophys. Acta* **1838,** 2484–2491
32. Cereijido, M., Robbins, E. S., Dolan, W. J., Rotunno, C. A., and Sabatini, D. D. (1978) Polarized monolayers formed by epithelial cells on a permeable and translucent support. *J. Cell Biol.* **77,** 853–880
33. Fahlke, C., Desai, R. R., Gillani, N., and George, A. L. (2001) Residues lining the inner pore vestibule of human muscle chloride channels. *J. Biol. Chem.* **276,** 1759–1765
34. Stölting, G., Fischer, M., and Fahlke, C. (2014) ClC-1 and ClC-2 form hetero-dimeric channels with novel protopore functions. *Pflugers Arch.* **466,** 2191–2204
35. Nothmann, D., Leinenweber, A., Torres-Salazar, D., Kovermann, P., Hotzy, J., Gameiro, A., Grewer, C., and Fahlke, C. (2011) Hetero-oligomerization of neuronal glutamate transporters. *J. Biol. Chem.* **286,** 3935–3943
36. Feng, L., Campbell, E. B., Hsiung, Y., and MacKinnon, R. (2010) Structure of a eukaryotic CLC transporter defines an intermediate state in the transport cycle. *Science* **330,** 635–641
37. Miller, C. (1982) Open-state substructure of single chloride channels from Torpedo electroplax. *Philos. Trans. R. Soc. Lond. B. Biol. Sci.* **299,** 401–411
38. Weinberger, S., Wojciechowski, D., Sternberg, D., Lehmann-Horn, F., Jurkat-Rott, K., Becher, T., Begemann, B., Fahlke, C., and Fischer, M. (2012) Disease-causing mutations C277R and C277Y modify gating of human ClC-1 chloride channels in myotonia congenita. *J. Physiol.* **590,** 3449–3464
39. Hayama, A., Rai, T., Sasaki, S., and Uchida, S. (2003) Molecular mechanisms of Bartter syndrome caused by mutations in the *BSND* gene. *Histochem. Cell Biol.* **119,** 485–493
40. Rickheit, G., Maier, H., Strenzke, N., Andreescu, C. E., De Zeeuw, C. I., Muenscher, A., Zdebik, A. A., and Jentsch, T. J. (2008) Endocochlear potential depends on Cl- channels: mechanism underlying deafness in Bartter syndrome IV. *EMBO J.* **27,** 2907–2917
41. Tajima, M., Hayama, A., Rai, T., Sasaki, S., and Uchida, S. (2007) Barttin binds to the outer lateral surface of the ClC-K2 chloride channel. *Biochem. Biophys. Res. Commun.* **362,** 858–864
42. Otsuka, M., Matsumoto, T., Morimoto, R., Arioka, S., Omote, H., and Moriyama, Y. (2005) A human transporter protein that mediates the final excretion step for toxic organic cations. *Proc. Natl. Acad. Sci. U.S.A.* **102,** 17923–17928
43. Lohi, H., Kujala, M., Mäkelä, S., Lehtonen, E., Kestilä, M., Saarialho-Kere, U., Markovich, D., and Kere, J. (2002) Functional characterization of three novel tissue-specific anion exchangers SLC26A7, -A8, and -A9. *J. Biol. Chem.* **277,** 14246–14254
44. Kieferle, S., Fong, P., Bens, M., Vandewalle, A., and Jentsch, T. J. (1994) Two highly homologous members of the ClC chloride channel family in both rat and human kidney. *Proc. Natl. Acad. Sci. U.S.A.* **91,** 6943–6947
45. L'Hoste, S., Diakov, A., Andrini, O., Genete, M., Pinelli, L., Grand, T., Keck, M., Paulais, M., Beck, L., Korbmacher, C., Teulon, J., and Lourdel, S. (2013) Characterization of the mouse ClC-K1/Barttin chloride channel. *Biochim. Biophys. Acta* **1828,** 2399–2409
46. Bateman, A. (1997) The structure of a domain common to archaebacteria and the homocystinuria disease protein. *Trends Biochem. Sci.* **22,** 12–13
47. Maduke, M., Williams, C., and Miller, C. (1998) Formation of CLC-0

chloride channels from separated transmembrane and cytoplasmic domains. *Biochemistry* **37,** 1315–1321
48. Hebeisen, S., Biela, A., Giese, B., Müller-Newen, G., Hidalgo, P., and Fahlke, C. (2004) The role of the carboxyl terminus in ClC chloride channel function. *J. Biol. Chem.* **279,** 13140–13147
49. Hebeisen, S., and Fahlke, C. (2005) Carboxy-terminal truncations modify the outer pore vestibule of muscle chloride channels. *Biophys. J.* **89,** 1710–1720
50. Garcia-Olivares, J., Alekov, A., Boroumand, M. R., Begemann, B., Hidalgo, P., and Fahlke, C. (2008) Gating of human ClC-2 chloride channels and regulation by carboxy-terminal domains. *J. Physiol.* **586,** 5325–5336
51. Stölting, G., Teodorescu, G., Begemann, B., Schubert, J., Nabbout, R., Toliat, M. R., Sander, T., Nürnberg, P., Lerche, H., and Fahlke, C. (2013) Regulation of ClC-2 gating by intracellular ATP. *Pflugers Arch.* **465,** 1423–1437
52. Schwappach, B., Stobrawa, S., Hechenberger, M., Steinmeyer, K., and Jentsch, T. J. (1998) Golgi localization and functionally important domains in the NH_2 and COOH terminus of the yeast CLC putative chloride channel Gef1p. *J. Biol. Chem.* **273,** 15110–15118
53. Ludwig, M., Doroszewicz, J., Seyberth, H. W., Bökenkamp, A., Balluch, B., Nuutinen, M., Utsch, B., and Waldegger, S. (2005) Functional evaluation of Dent's disease-causing mutations: implications for ClC-5 channel trafficking and internalization. *Hum. Genet.* **117,** 228–237
54. Carr, G., Simmons, N., and Sayer, J. (2003) A role for CBS domain 2 in trafficking of chloride channel CLC-5. *Biochem. Biophys. Res. Commun.* **310,** 600–605
55. Stauber, T., and Jentsch, T. J. (2010) Sorting Motifs of the Endosomal/Lysosomal CLC Chloride Transporters. *J. Biol. Chem.* **285,** 34537–34548
56. Lange, P. F., Wartosch, L., Jentsch, T. J., and Fuhrmann, J. C. (2006) ClC-7 requires Ostm1 as a β-subunit to support bone resorption and lysosomal function. *Nature* **440,** 220–223
57. Cleiren, E., Bénichou, O., Van Hul, E., Gram, J., Bollerslev, J., Singer, F. R., Beaverson, K., Aledo, A., Whyte, M. P., Yoneyama, T., deVernejoul, M.-C., and Van Hul, W. (2001) Albers-Schönberg disease (autosomal dominant osteopetrosis, type II) results from mutations in the *ClCN7* chloride channel gene. *Hum. Mol. Genet.* **10,** 2861–2867
58. Simons, K., and Fuller, S. D. (1985) Cell surface polarity in epithelia. *Annu. Rev. Cell Biol.* **1,** 243–288
59. Keck, M., Andrini, O., Lahuna, O., Burgos, J., Cid, L. P., Sepúlveda, F. V., L'Hoste, S., Blanchard, A., Vargas-Poussou, R., Lourdel, S., and Teulon, J. (2013) Novel *CLCNKB* mutations causing Bartter syndrome affect channel surface expression. *Hum. Mutat.* **34,** 1269–1278
60. Nomura, N., Tajima, M., Sugawara, N., Morimoto, T., Kondo, Y., Ohno, M., Uchida, K., Mutig, K., Bachmann, S., Soleimani, M., Ohta, E., Ohta, A., Sohara, E., Okado, T., Rai, T., Jentsch, T. J., Sasaki, S., and Uchida, S. (2011) Generation and analyses of R8L barttin knockin mouse. *Am. J. Physiol. Renal Physiol.* **301,** F297–F307
61. Martinez, G. Q., and Maduke, M. (2008) A cytoplasmic domain mutation in ClC-Kb affects long-distance communication across the membrane. *PLoS ONE* 10.1371/journal.pone.0002746
62. Liantonio, A., Picollo, A., Babini, E., Carbonara, G., Fracchiolla, G., Loiodice, F., Tortorella, V., Pusch, M., and Camerino, D. C. (2006) Activation and inhibition of kidney CLC-K chloride channels by fenamates. *Mol. Pharmacol.* **69,** 165–173
63. Nomura, N., Kamiya, K., Ikeda, K., Yui, N., Chiga, M., Sohara, E., Rai, T., Sakaki, S., and Uchida, S. (2013) Treatment with 17-allylamino-17-demethoxygeldanamycin ameliorated symptoms of Bartter syndrome type IV caused by mutated Bsnd in mice. *Biochem. Biophys. Res. Commun.* **441,** 544–549
64. Andrini, O., Keck, M., L'Hoste, S., Briones, R., Mansour-Hendili, L., Grand, T., Sepúlveda, F. V., Blanchard, A., Lourdel, S., Vargas-Poussou, R., and Teulon, J. (2013) CLCNKB mutations causing mild Bartter syndrome profoundly alter the pH and Ca2+ dependence of ClC-Kb channels. *Pflugers Arch.* **466,** 1713–1723